Supporting information for ACS Nano

Artificial Nano-Targeted Cells (ANTC) with Stable Photothermal Performance for Multimodal Imaging-Guided Tumor-Specific Therapy

Bin Qiao[1#], Yuanli Luo[1#], Hong-Bo Cheng[2], Jianli Ren[1], Jin Cao[1], Chao Yang[3], Bing Liang[1], Anyu Yang[1], Xun Yuan[1], Jinrui Li[1], Liming Deng[1], Pan Li[1], Hai-Tao Ran[1], Lan Hao[1], Zhiyi Zhou[4], Maoping Li[5], Yuanyuan Zhang[6], Peter S. Timashev[7], Xing-Jie Liang[8,9], Zhigang Wang[1]**

1 Department of Ultrasound, Chongqing Key Laboratory of Ultrasound Molecular Imaging, the Second Affiliated Hospital of Chongqing Medical University, Chongqing 400010, P. R. China

2 State Key Laboratory of Organic-Inorganic Composites, Beijing Laboratory of Biomedical Materials, Beijing University of Chemical Technology, Beijing 100029, P. R. China

3 Department of Radiology, Chongqing General Hospital of Chinese Academy of Sciences Chongqing 400014, P. R. China

4 Department of General Medicine, Chongqing General Hospital of Chinese Academy of Sciences, Chongqing 400014, P. R. China

5 Department of Ultrasound, the First Affiliated Hospital of Chongqing Medical University, Chongqing 400010, P. R. China

6 Wake Forest Institute for Regenerative Medicine, Wake Forest University School of Medicine, Winston-Salem, North Carolina 27101-4135, USA.

7 Institute for Regenerative Medicine, Sechenov University, Moscow 119991, Russia

8 CAS Key Laboratory for Biomedical Effects of Nanomaterials and Nanosafety, CAS Center for Excellence in Nanoscience, National Center for Nanoscience and Technology of China, Beijing 100190, P. R. China

9 University of Chinese Academy of Sciences, Beijing 100049, P. R. China.

[#]These authors contributed equally to this work.

*To whom correspondence may be addressed: wzg62942443@163.com (Zhigang Wang), liangxj@nanoctr.cn (Xing-Jie Liang)

Contents

A: Experimental Section.

Photothermal Conversion Efficiency of MPFTNPs: According to the method reported by Roper's team, the η of MPFTNPs was calculated.[1-2] Briefly, 200 μL of MPFTNPs suspension was added to 96-well plates and irradiation was performed with an 808 nm laser at an intensity of 2.0 W cm^{-2}. Then, the laser was turned off after the temperature reached a steady state. The heating and cooling process was recorded using an infrared thermal imaging camera. The η of MPFTNPs was calculated according to the following formulas:

$$(1)\quad \eta = \frac{hS\Delta T_{Max} - Q_S}{I(1-10^{-A_\lambda})}$$

$$(2)\quad \tau_s = \frac{\sum_i m_i c_{pi}}{hS}$$

In formula 1, η represents the conversion efficiency value, ΔT_{max} is the maximum equilibrium temperature minus the minimum equilibrium temperature, *Qs* is the light absorbance of distilled water, *I* is the laser energy (mW) for the 808 nm laser, and A_λ is related to the absorbance value of the MPFTNP suspension tested by analysis of the UV-Vis spectrum at 808 nm. The value of *hS* was calculated based on formula 2.

In formula 2, m represents the mass of water (200 mg), and C represents the specific heat capacity (4.2 J g^{-1} K^{-1}). The time constant (τs) was calculated from the linear time-dependent data collected in the cooling period (Figure 2H) and determined to be 213.3 s. According to the formula (2), the hS was calculated to be 3.938×10^{-3} W K^{-1}.

Finally, the η of MPFTNPs was calculated based on formula 1. The ΔT_{max} value of MPFTNPs was 33.0 °C under pH 4.5, the ΔT_{max} value of PFTNPs was 20.4 °C under pH 4.5, *Qs* was measured to be 1.68 mW, and *I* was determined to be 0.64 mW. A_λ was determined to be 0.49 as tested by UV-Vis spectroscopy at 808 nm. The η of MPFTNPs (pH 4.5) under 808 nm laser irradiation was calculated to be 30.02%. The η of PFTNPs (pH 4.5) under 808 nm laser irradiation was calculated to be 18.56%.

Calculation of Combination index (CI) of PDT and PTT: The CI is calculated by the following Equation:

$$CI = \frac{D_{A|A+B}}{DA} + \frac{D_{B|A+B}}{DB} = 0.703$$

In the above equation, $D_{A|A+B}$and $D_{B|A+B}$ are the IC50 doses (the half-maximal inhibitory concentration) for PDT and PTT in combined therapy, respectively. D_A is the IC50 dose for PDT and D_B is the IC50 dose for PTT against MDA-MB-231 cells. The CI value reflects the interaction effect between PDT and PTT. CI < 0.6 indicates strong synergism; 0.6 < CI < 0.8 indicates moderate synergism; 0.8 < CI < 0.9 indicates slight synergism; while 0.9 < CI < 1.1 indicates an additive effect according to the previous report. [3-4]

B: Supplementary figures

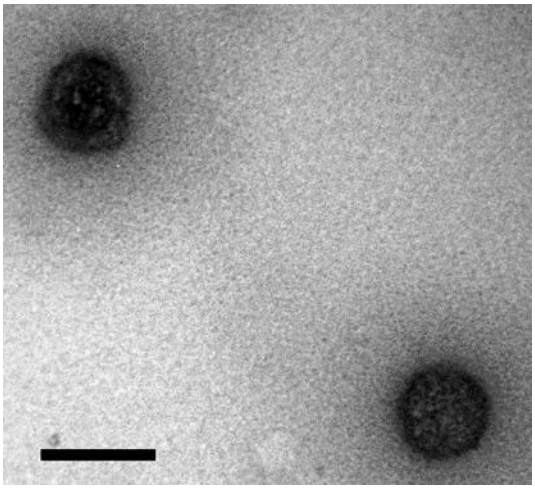

Figure S1. TEM image of PFTNPs. The scale bar is 200 nm.

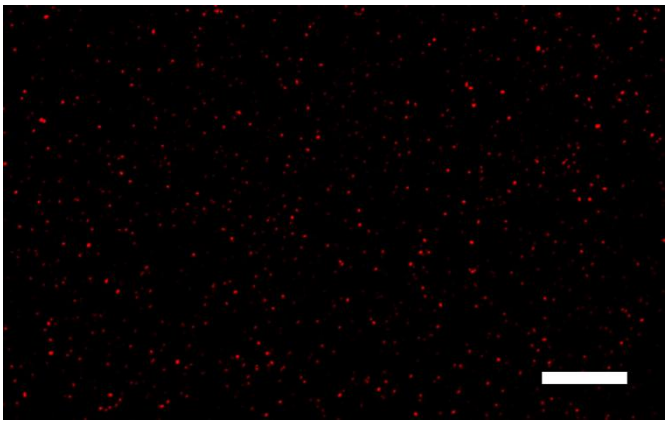

Figure S2. CLSM image of MPFTNPs (λexcitation/λemission = 635 nm/680 nm.). The scale bar is 20 μm.

Figure S3. Digital images of PFTNPs (left) and MPFTNPs (right).

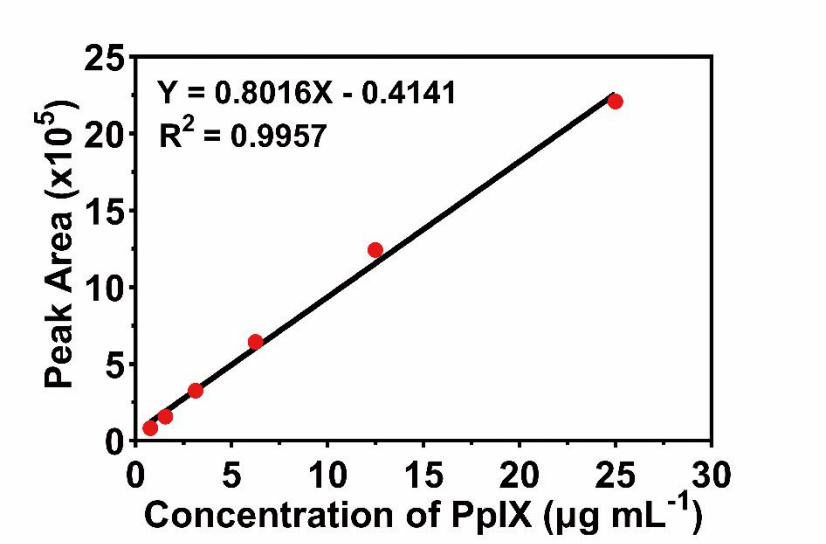

Figure S4. Standard curve of PpIX based on high-performance liquid chromatography (HPLC).

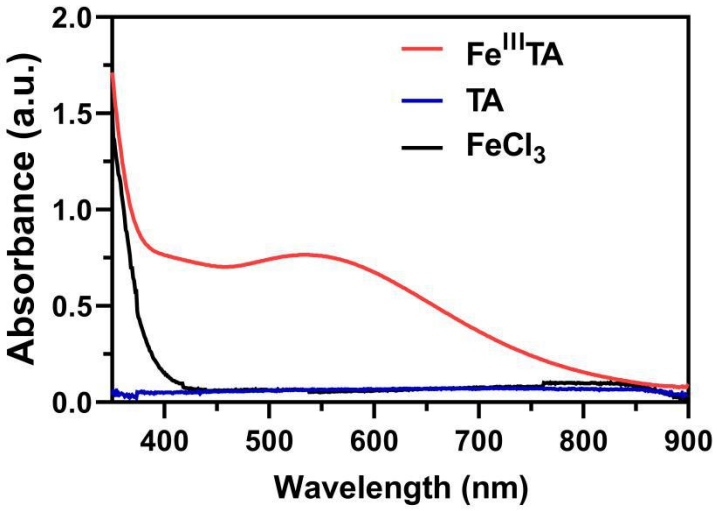

Figure S5. The UV-vis spectrum of TA, $FeCl_3$, and $Fe^{III}TA$.

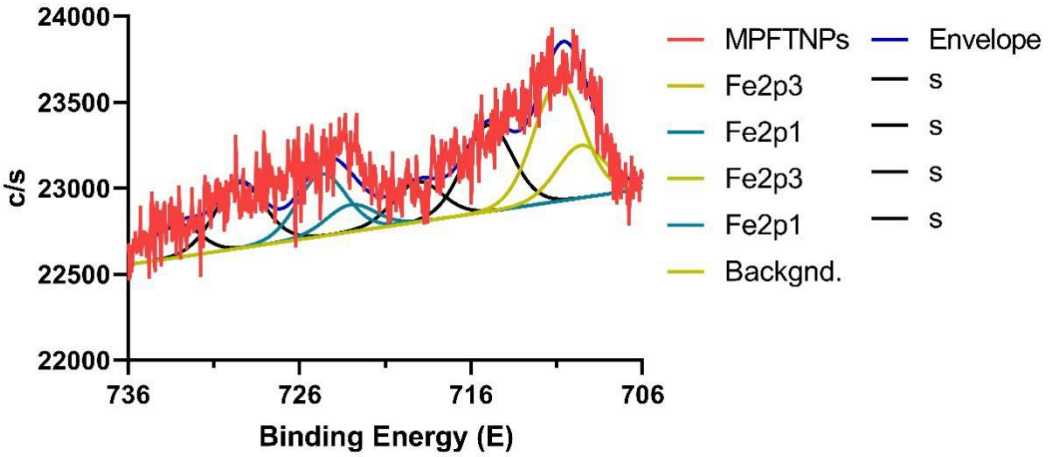

Figure S6. XPS high-resolution Fe2p spectra of MPFTNPs.

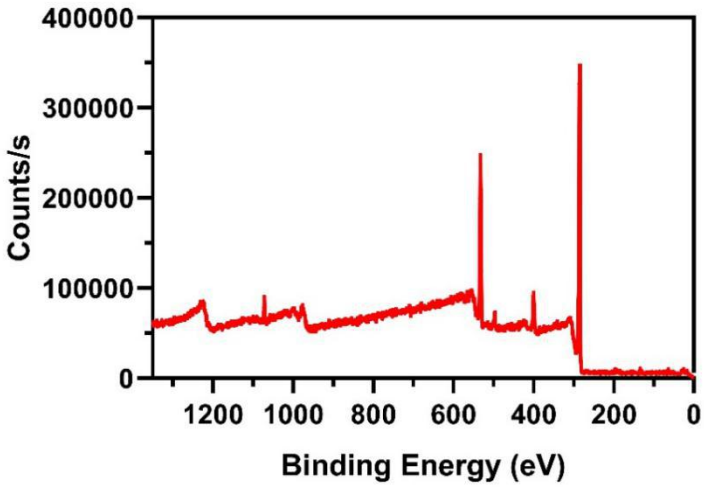

Figure S7. XPS spectra of MPFTNPs.

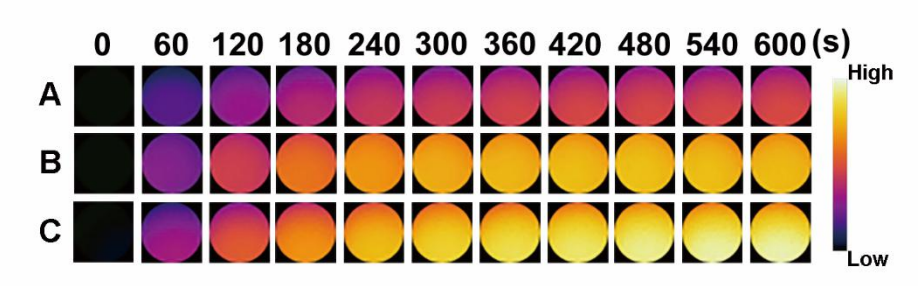

Figure S8. Infrared thermal images of PFTNPs under 808 nm laser irradiation with different pH values at a power density of 2.0 W cm^{-2} (A: pH 4.5; B: pH 5.5; C: pH 7.0).

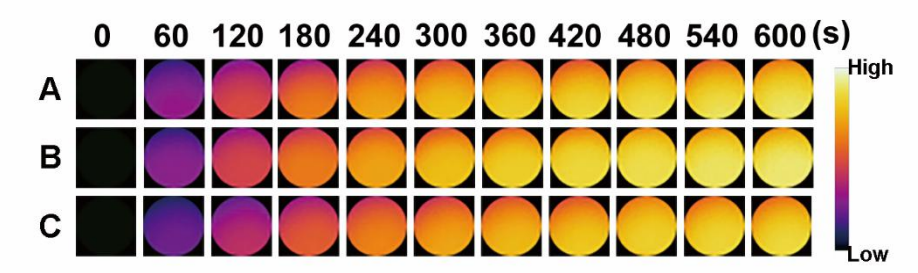

Figure S9. Infrared thermal images of MPFTNPs under 808 nm laser irradiation with different pH values at a power density of 2.0 W cm^{-2} (A: pH 7.0; B: pH 5.5; C: pH 4.5).

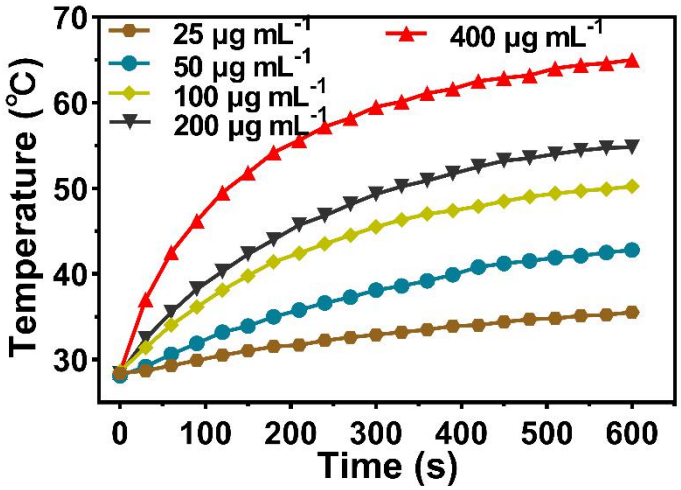

Figure S10. Photothermal curves of MPFTNPs at various concentrations.

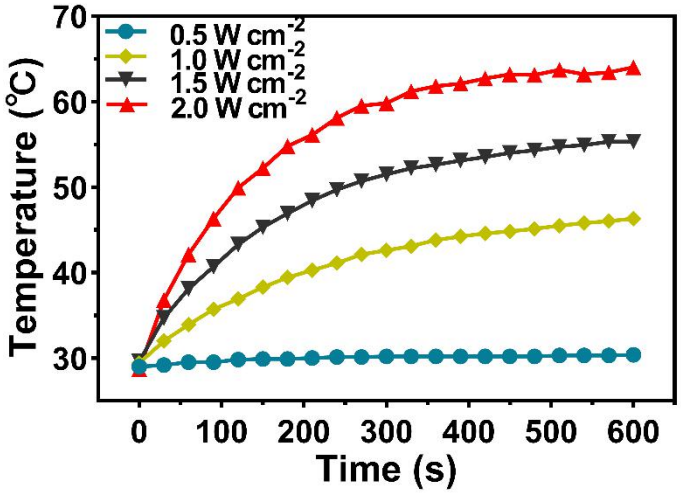

Figure S11. Photothermal curves of MPFTNPs at different laser power densities.

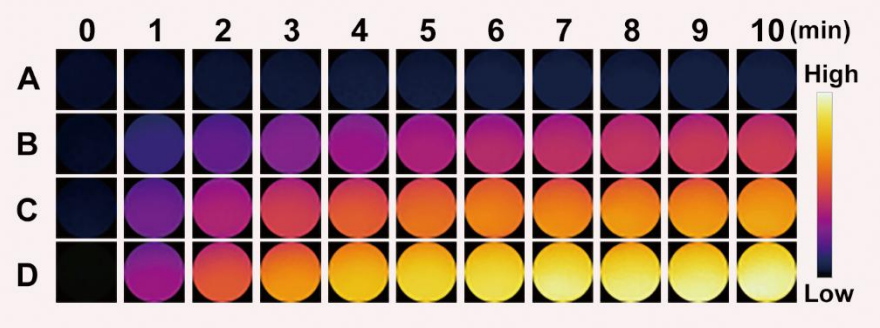

Figure S12. Infrared thermal images under irradiation with different laser power densities (A: 0.5 W cm^{-2}, B: 1.0 W cm^{-2}, C: 1.5 W cm^{-2}, D: 2.0 W cm^{-2}).

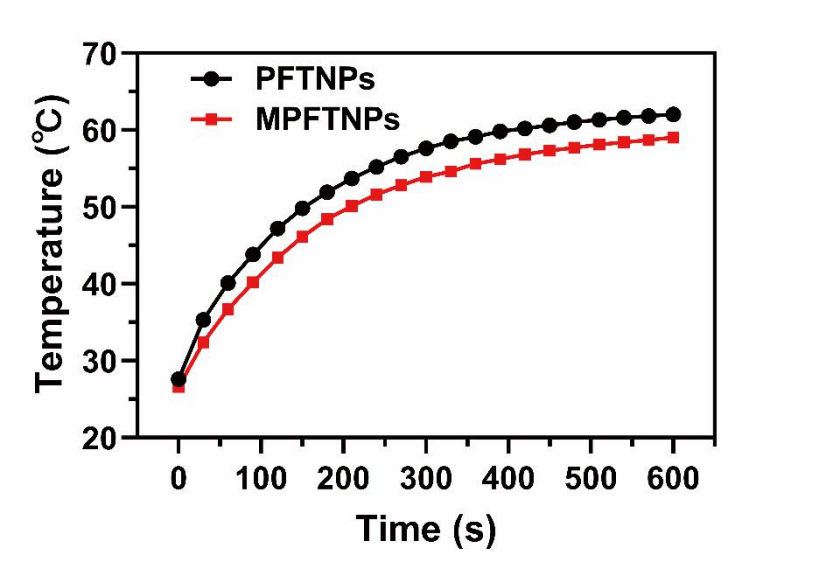

Figure S13. Photothermal performance of MPFTNPs and PFTNPs under 808 nm laser irradiation for 10 min.

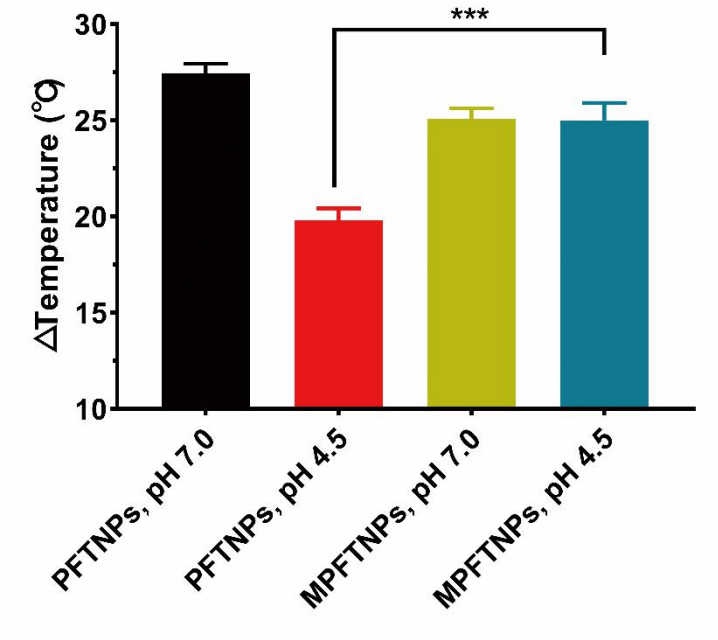

Figure S14. Temperature change in PFTNPs and MPFTNPs at 8 h of incubation under different pH.

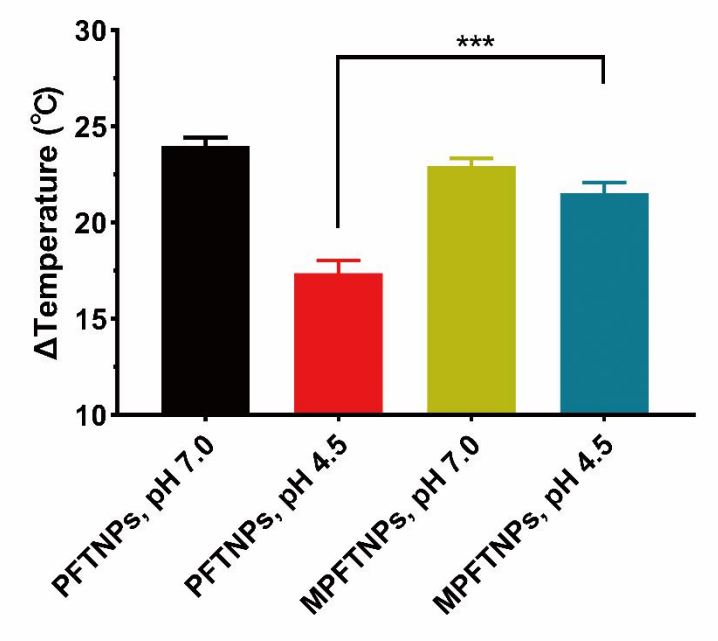

Figure S15. Temperature change in PFTNPs and MPFTNPs at 24 h of incubation under different pH.

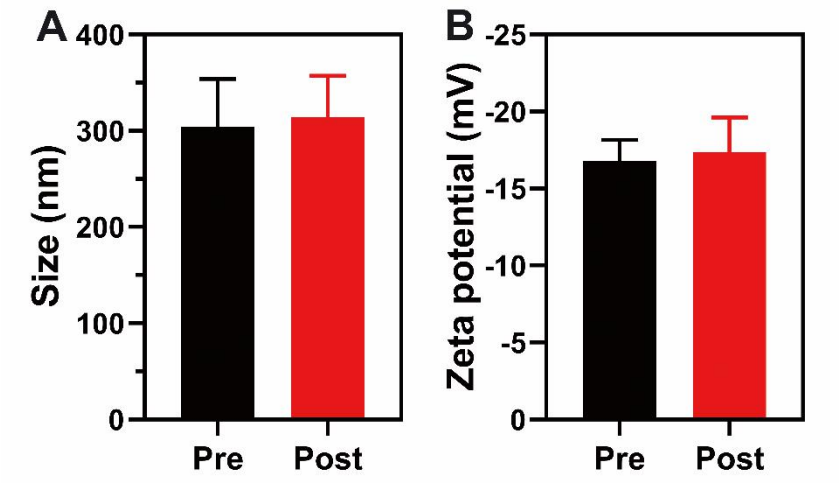

Figure S16. (A) Size and (B) Zeta potential change after 5 cycles of PTT.

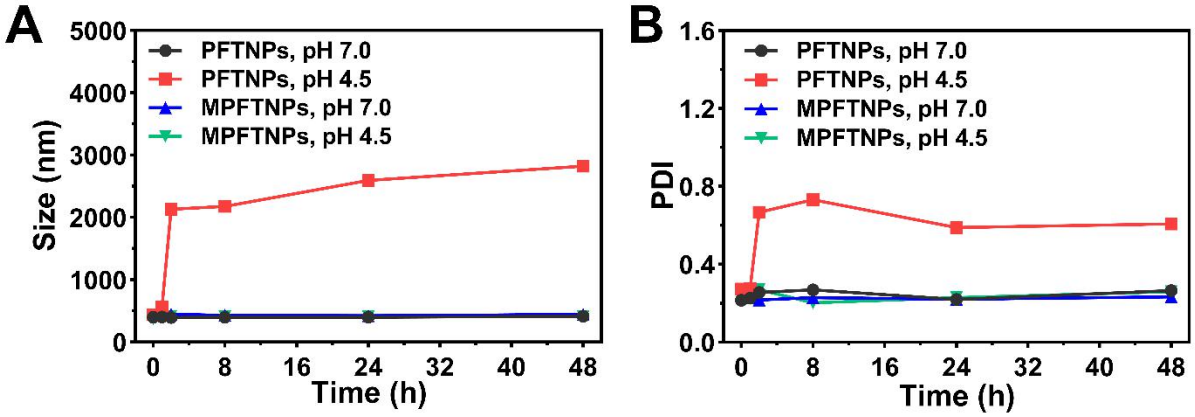

Figure S17. (A) The Size and (B) PDI change of PFTNPs and MPFTNPs in pH 4.5 or pH 7.0 after incubation.

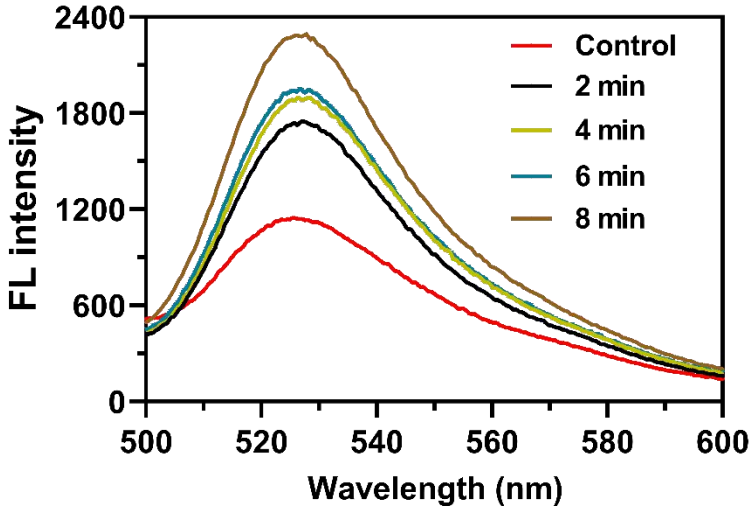

Figure S18. SOSG fluorescence intensity of MPFTNPs. Time-dependent ROS production of MPFTNPs as irradiated by 660 nm laser (0.1 W cm^{-2}). The concentration of PpIX was 15 μg mL^{-1}.

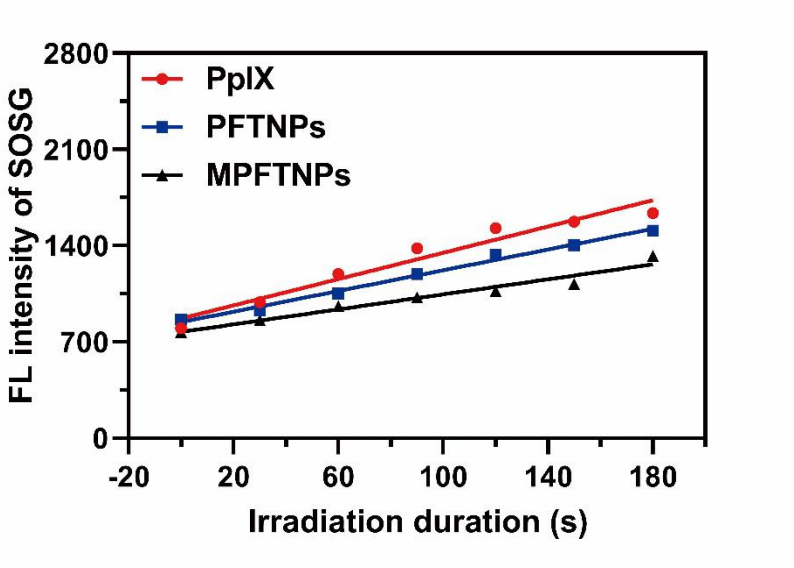

Figure S19. ROS production in solutions as determined by SOSG. The concentration of PpIX was 10 μg mL^{-1}.

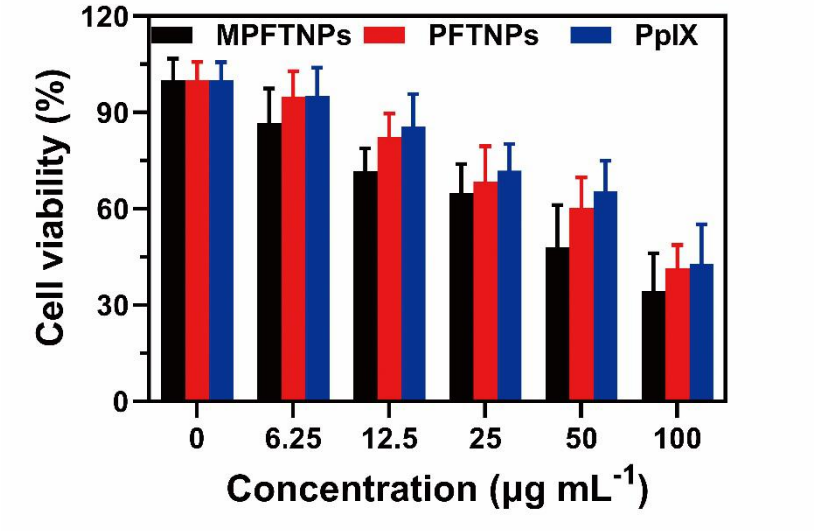

Figure S20. Cell viability of MDA-MB-231 cells treated with MPFTNPs, PFTNPs, and PpIX with 660 nm laser irradiation (100 mW cm^{-2}, 3 min).

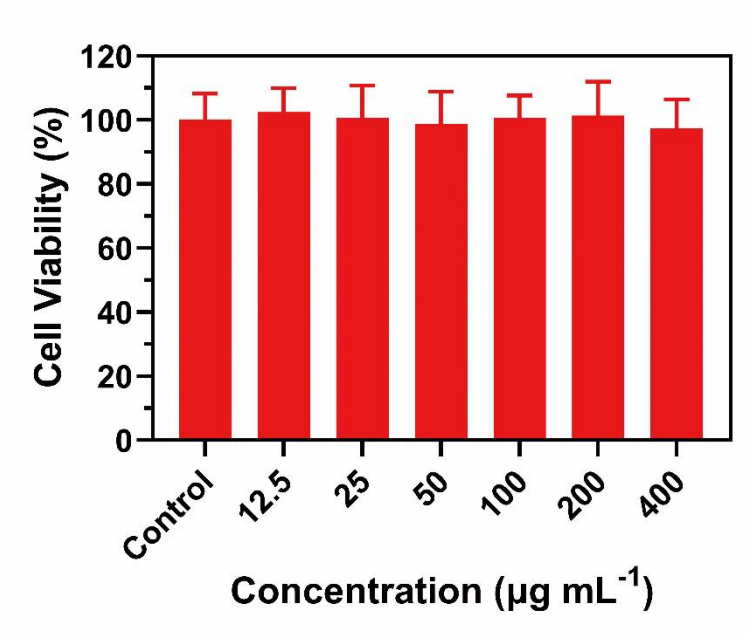

Figure S21. Viability of MDA-MB-231 cells after coincubation with various concentrations of the cancer cell membrane.

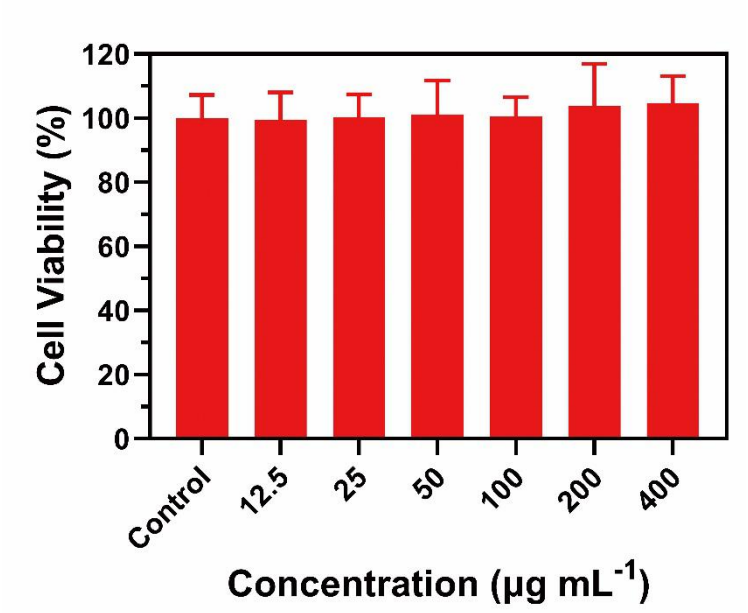

Figure S22. Viability of MDA-MB-231 cells after coincubation with various concentrations of $Fe^{III}TA$.

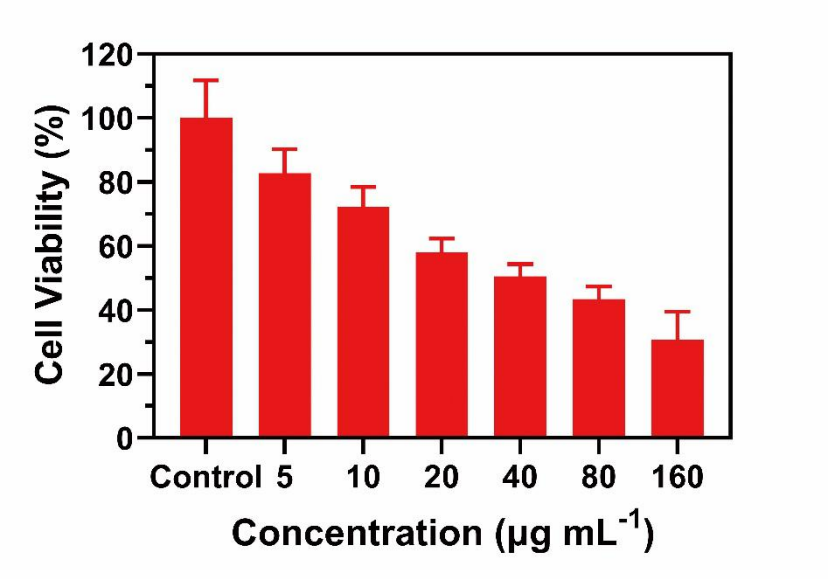

Figure S23. Viability of MDA-MB-231 cells after coincubation with various concentrations of free PpIX.

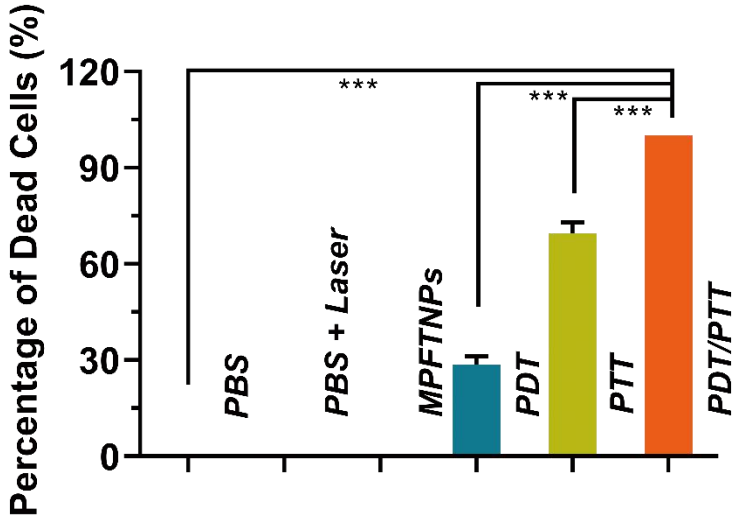

Figure S24. Quantitative analysis of MDA-MB-231 cells costained with calcein AM (living cells, green) and propidium iodide (dead cells, red) after various treatments according to CLSM.

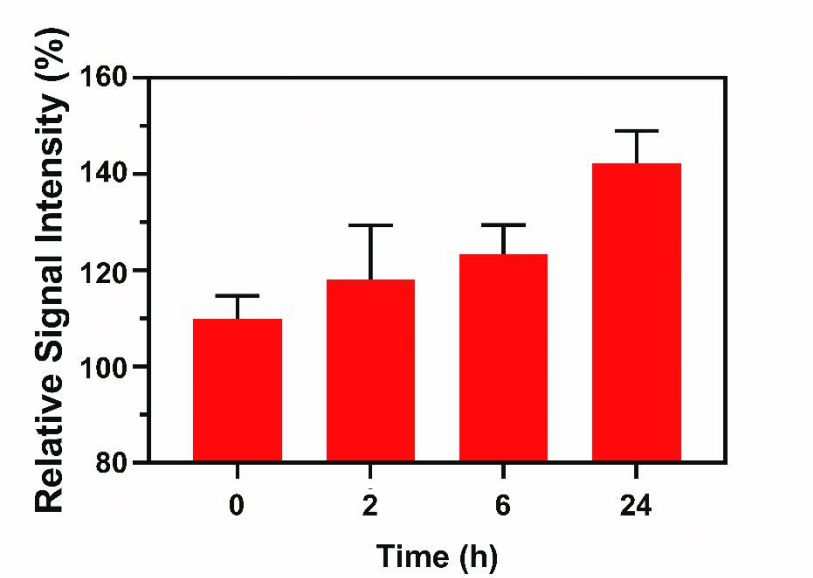

Figure S25. Quantitative analysis of MRI signals at the tumor site relative to liver tissue.

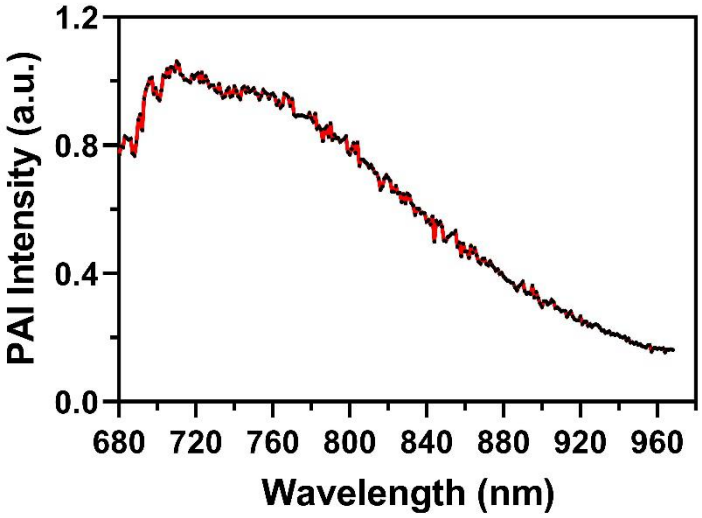

Figure S26. PAI intensity under full-spectrum scanning (ranging from 680 to 968 nm).

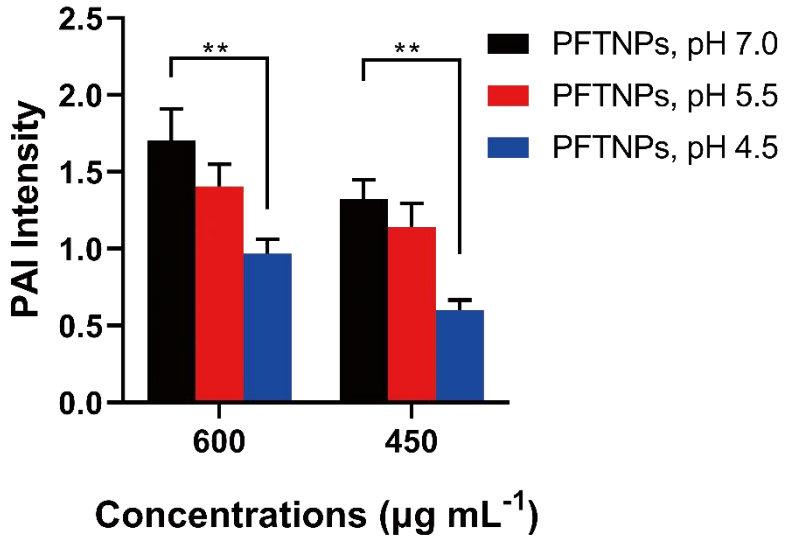

Figure S27. PAI intensity values of PFTNPs under different pH.

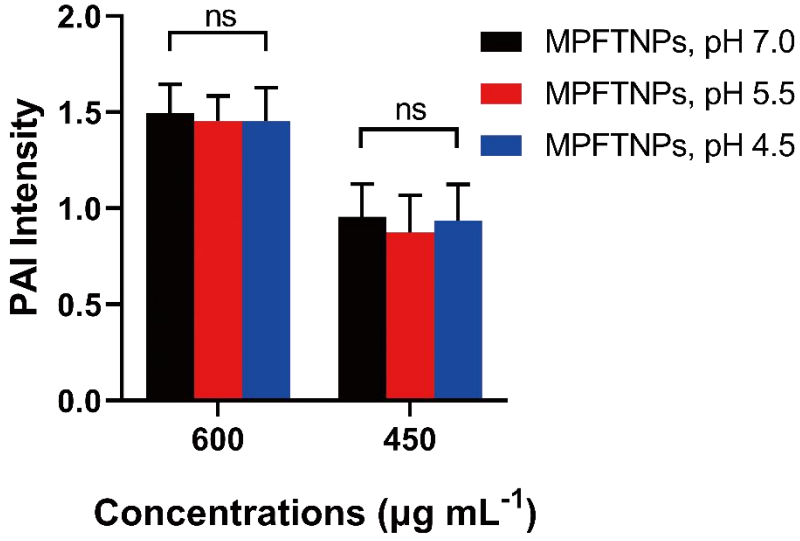

Figure S28. PAI intensity values of MPFTNPs under different pH.

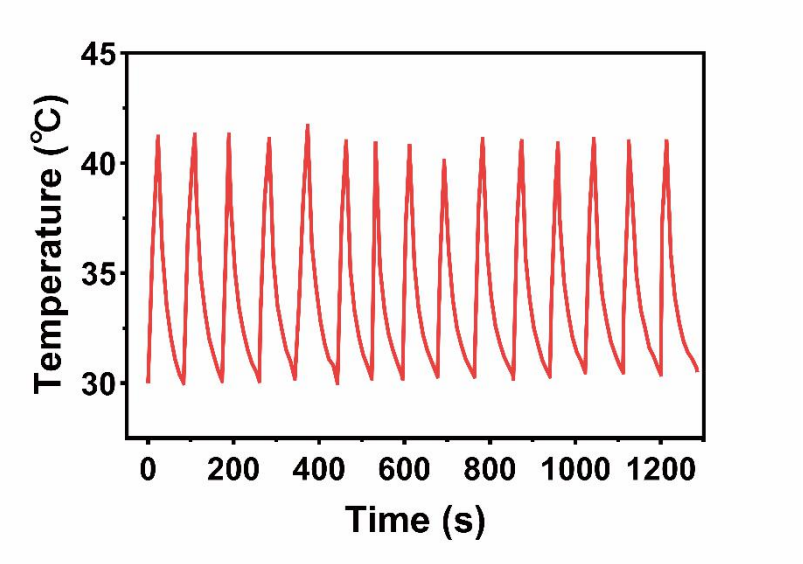

Figure S29. Temperature changes during the PDT process *in vivo*.

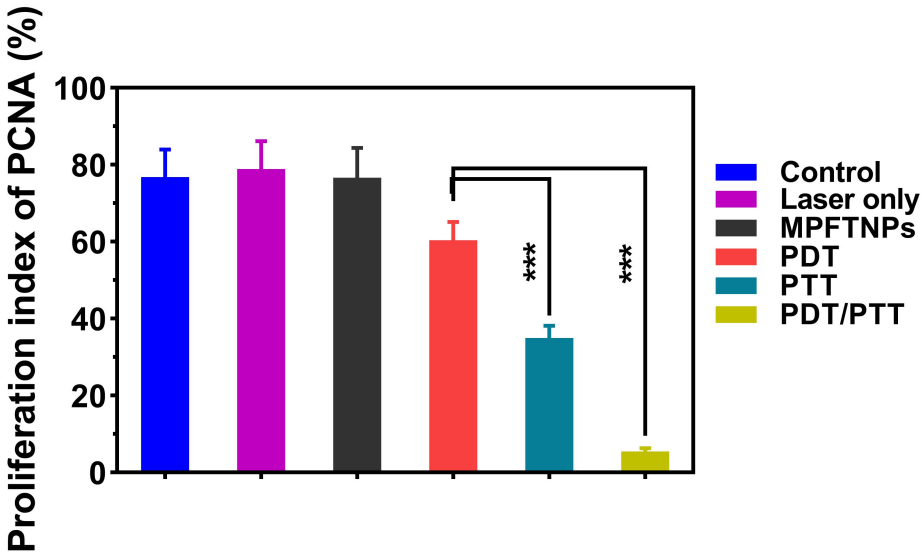

Figure S30. Quantitative analysis of the proliferation index in different groups.

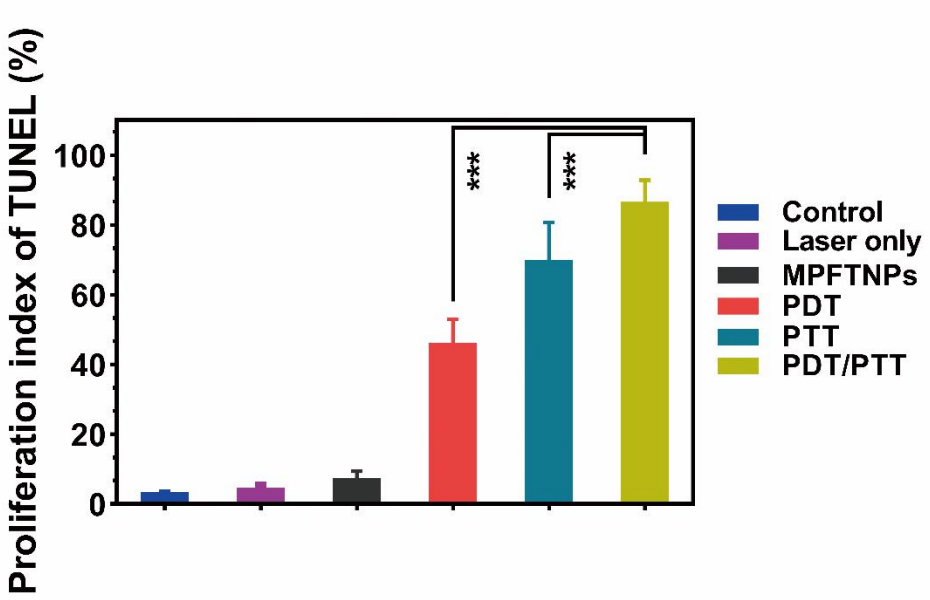

Figure S31. Quantitative analysis of the apoptotic index in different groups.

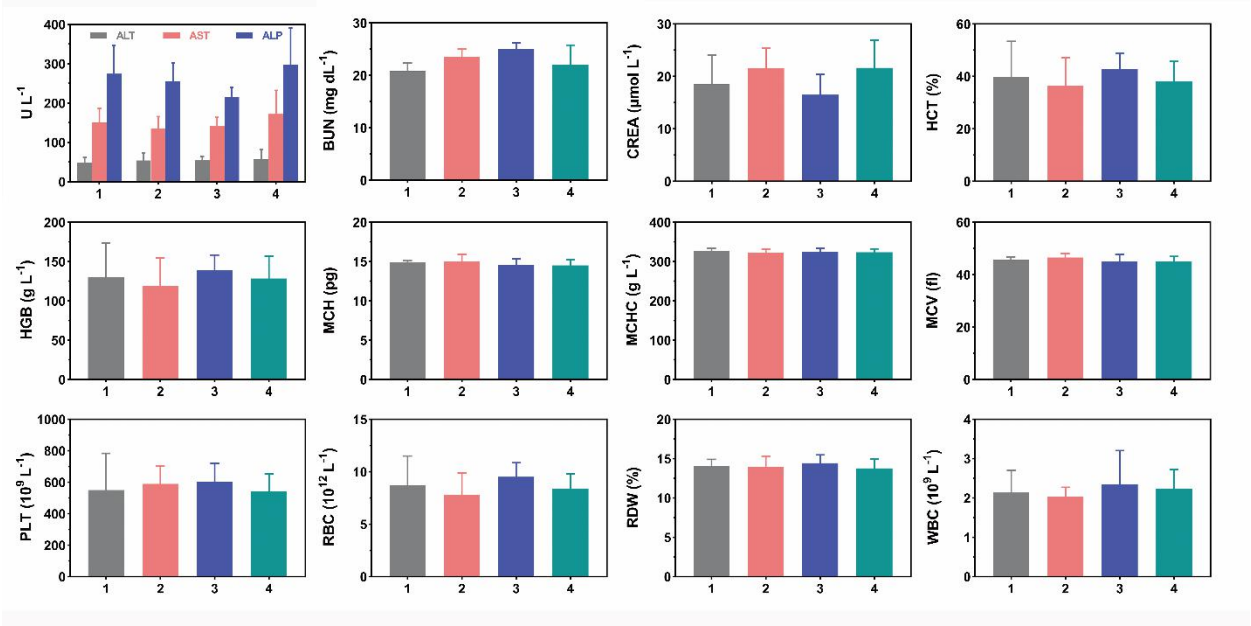

Figure S32. Hematological assays of mice sacrificed 30 d post injection of MPFTNPs at different concentrations (group 1: 0 mg mL^{-1}, group 2: 10 mg mL^{-1}, group 3: 20 mg mL^{-1}, and group 4: 40 mg mL^{-1}). There was no significant difference between the groups.

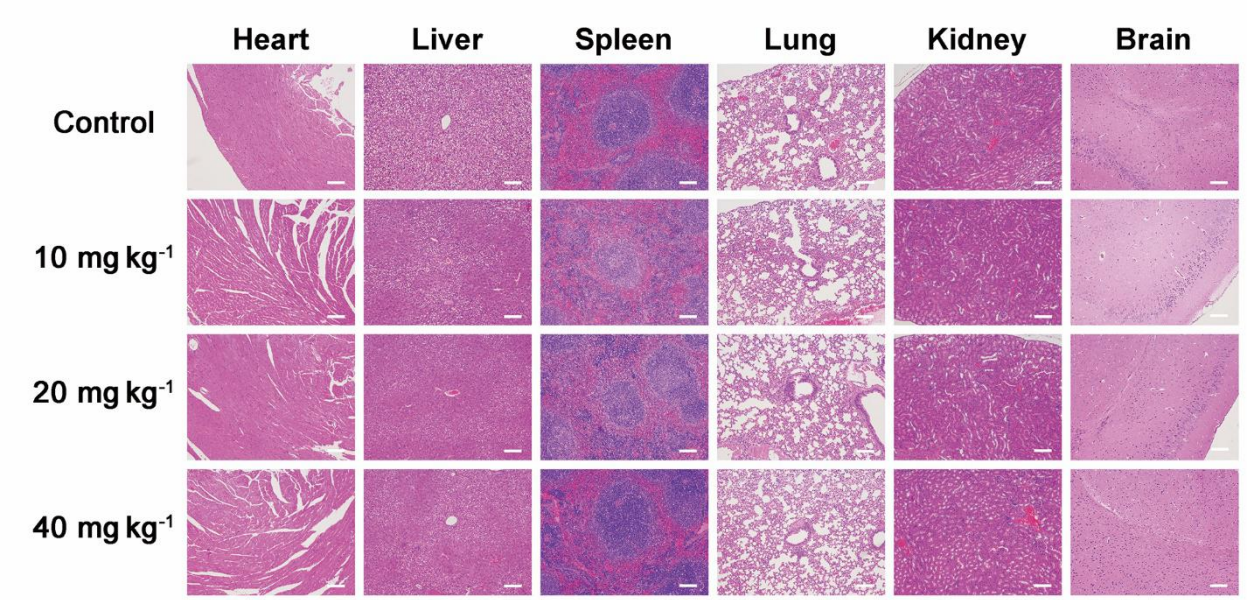

Figure S33. Hematoxylin & eosin (H&E) staining of the heart, liver, spleen, lungs, kidneys, and brain in mice sacrificed 30 d post injection of MPFTNPs at different concentrations (0, 10, 20, and 40 mg mL^{-1}). The scale bar is 100 μm.

C. Supplementary Tables.

	PFTNPs	MPFTNPs
pH 7.0	32.39%	31.93%
pH 5.5	23.38%	31.11%
pH 4.5	18.56%	30.02%

Table S1. Photothermal conversion efficiency of MPFTNPs and PFTNPs under different pH.

References:

1. Feng, W.; Han, X.; Wang, R.; Gao, X.; Hu, P.; Yue, W.; Chen, Y.; Shi, J., Nanocatalysts-Augmented and Photothermal-Enhanced Tumor-Specific Sequential Nanocatalytic Therapy in Both NIR-I and NIR-II Biowindows. *Adv. Mater.* **2019**, *31*, e1805919.

2. Liu, T.; Zhang, M.; Liu, W.; Zeng, X.; Song, X.; Yang, X.; Zhang, X.; Feng, J., Metal Ion/Tannic Acid Assembly as a Versatile Photothermal Platform in Engineering Multimodal Nanotheranostics for Advanced Applications. *ACS Nano* **2018**, *12*, 3917-3927.

3. Cheng, L.; Zhang, F.; Wang, S.; Pan, X.; Han, S.; Liu, S.; Ma, J.; Wang, H.; Shen, H.; Liu, H.; Yuan, Q., Activation of Prodrugs by NIR-Triggered Release of Exogenous Enzymes for Locoregional Chemo-Photothermal Therapy. *Angew. Chem. Int. Ed. Engl.* **2019**, *58*, 7728-7732.

4. Barua, S.; Mitragotri, S., Synergistic Targeting of Cell Membrane, Cytoplasm, and Nucleus of Cancer Cells Using Rod-Shaped Nanoparticles. *ACS Nano* **2013**, *7,* 9558-9570.